Application of 3D AE Tomography for Triaxial Tests of Rocky Specimens

Tomoki SHIOTANI*, Satoshi OSAWA*, Yoshikazu KOBAYASHI**, Shohei MOMOKI***
* Graduate School of Engineering, Kyoto University, Kyoto, Japan
E-mail: shiotani.tomoki.3v@kyoto-u.ac.jp, oosawa.satoshi.88w@st.kyoto-u.ac.jp, respectively
** College of Science and Technology, Nihon University, Tokyo, Japan
E-mail: kobayasi@civil.cst.nihon-u.ac.jp
*** Research Institute of Technology, Tobishima Corporation, Chiba, Japan
E-mail: shouhei_momoki@tobishima.co.jp

Abstract. Preventive maintenance is of high demand for managing existent infrastructures with the reasonable procedure including life cycle cost [1]. NDT approaches to diagnose the early internal damage of structures have thus been studied extensively. In order to respond to these issues, the authors had proposed 'AE tomography' which executes both of AE monitoring and elastic wave tomography and succeeded to apply the diagnosis of planar structures [2]. The AE tomography enables to provide accurate AE source locations as well as the velocity distribution with the tomography simultaneously. In this paper, newly developed 3D AE tomography will be briefly introduced followed by the application of triaxial rock shear test. Through the application the applicability of 3D AE tomography [3] for diagnosis of actual deterioration/ damages of infrastructures will be discussed.

1. Introduction

In recent years, a lot of accidents of infrastructures frequency occur in Japan due to the deterioration, while as the working population is remarkably shrinking, the construction investment has been decreased year after year. Therefore it is important to repair and reinforce the infrastructures reasonably with the limited budget. There are two concepts for the maintenance strategies: reactive maintenance and preventive maintenance. The preventive maintenance, where the repair program has been implemented for their early damage stage, is considered the best method to expand their service life as long as possible with the limited charge. To implement the preventive maintenance program, the technique to investigate the early defect is thus in high demand. Conventionally NDT such as ultrasonic technique, an X-rays method and optical fiber sensing technology have been applied for the evaluation of the early internal damage; however, there exist issues to solve with respect to the range of application and the sensitivity of early damage. To examine these issues, our group had proposed 2D AE tomography, which can quantify the infrastructures' deterioration from micro to macro cracks. As one of the materials applied, the applicability of the AE tomography for rock materials was verified two dimensionally in our past studies [4, 5].

The principle contribution of this paper is to verify the applicability of 3D AE tomography, which is newly developed by our group with application of the same rock material as of 2Ds' past studies.

2. AE Tomography

2.1 AE Monitoring and Elastic Wave Tomography

AE tomography consists of AE monitoring and elastic wave tomography. Figures 1 and 2 show the configurations of AE monitoring and elastic wave tomography, respectively. AE monitoring is the method to determine the AE source location by using arrival time differences among AE sensors, where AE sources were generated due to the crack occurrence by load applications. The conventional AE source locations are conducted assuming elastic wave velocity of the structure being homogeneous; however, in civil engineering materials or failure-progressed materials, the velocity was not distributed uniformly due to materials' heterogeneity. Therefore the AE source locations are not always accurate in actual structures or materials in which the velocity does not exhibit homogeneous or the failure evolves successively. Accordingly the elastic wave tomography is well used, following the AE monitoring in many cases. The elastic wave tomography is the method to evaluate the distribution of elastic wave velocity over the structures. In the principle procedure, elastic wave is excited at the specific location near the sensor as to provide the excitation time for the first, and the elastic waves excited were to be received by other transducers (AE sensors). In this way, both the excitation time and the time of arrivals in all of the sensors can be obtained. In order to obtain the individual velocity over the structures, the structures are divided into some cells in advance. Initially, elastic wave velocity is assumed to be equal in each cell. Then it can be possible to calculate the elastic wave velocity of each cell by using both excitation time and the time of arrivals in all of the sensors. In addition, elastic wave tomography can transmit more waves artificially compared with AE monitoring, so that we can get more information about excitation time and the time of arrivals, leading to more accurate estimation of velocity distributions. Therefore elastic wave tomography is known as a highly precise method.

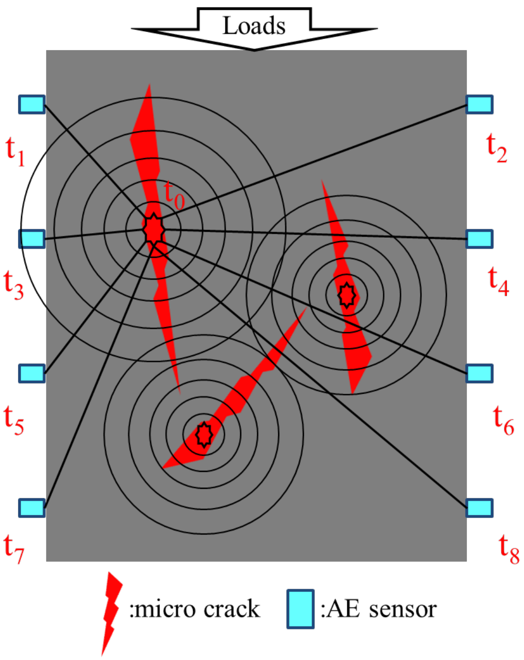

Fig. 1. AE monitoring

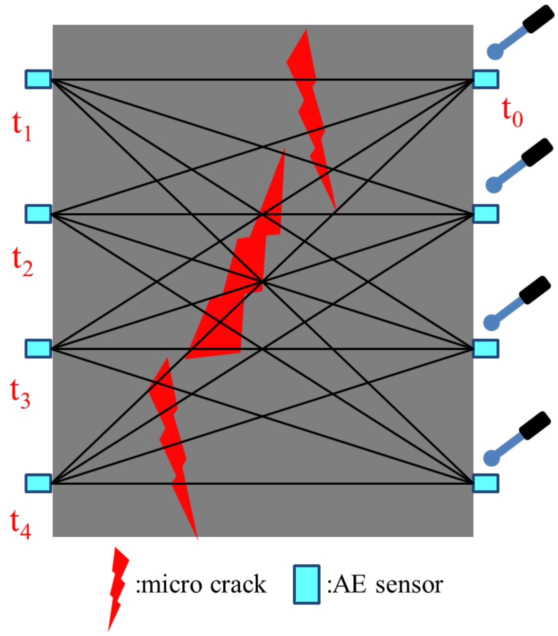

Fig. 2. Elastic wave tomography

2.2 2D AE Tomography

As shown above, it has been necessary for examining internal damages with high accuracy to use both AE monitoring and elastic wave tomography so far, while this led to a lot of time and cost to assess the structures. In order to solve this issue, our group had proposed '2D AE tomography' which implements AE monitoring and elastic wave tomography simultaneously [6]. Figure 3 shows the configuration of 2D AE tomography.

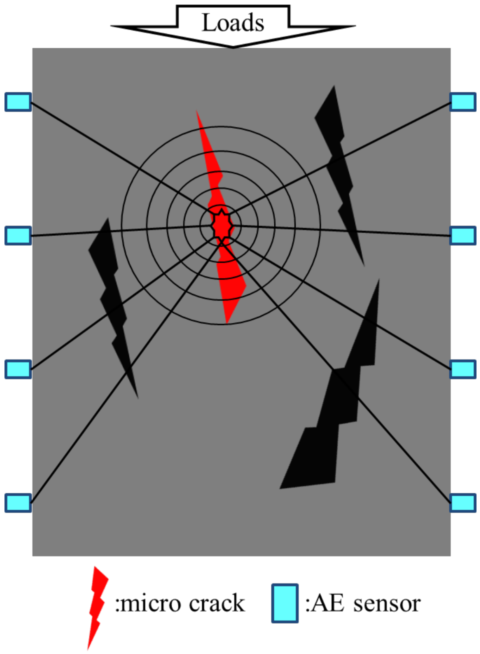

Fig. 3. The configuration of 2D AE tomography

The 2D AE tomography does not use elastic wave excited artificially, but utilizes AE waves generated within structures e.g., with load applications. It is possible to obtain the excitation time in the elastic wave tomography; however, it is impossible to get the generation time of AE waves in AE tomography, so that the estimation of generation time of all AE waves is essential for the first.

As shown in Figs. 4 and 5, in 2D AE tomography, the structure is divided into some elements, which consist of three cell nodes forming triangular shapes each other. In addition, each element is divided into smaller parts to increase source location candidates, being referred to as relay points as shown in Fig. 5. Again, both of cell nodes and relay points are the candidate for AE sources. Figure 4 also shows a configuration of ray-trace technique. As shown in Fig. 4, firstly, theoretical propagation time: T_{ij} is calculated each other from receiver point: j to all cell nodes: i and relay points. Then, T_j which defines the difference between the obtained time of arrivals and theoretical propagation time: T_{ij} in receiver point: j is calculated. Then the above process is conducted in each location of receiver (from receiver 1 to receiver n). And, by means of Eqs. 1 and 2, source locations showing the smallest variance are identified.

$$T_{im} = \frac{\sum_j (T_{ij} - T_j)}{N} \tag{1}$$

$$\sigma_{im} = \frac{\sum_j (T_{ij} - T_j - T_{im})^2}{N} \tag{2}$$

where T_{im} is average of estimated occurrence time and σ_{im} is variance of estimated occurrence time in the case of nodal point: *i*.

Based on the renewed AE source locations, the elastic wave velocity of each element is updated. This process is the one cycle for getting renewed both of AE source locations and elastic wave velocity. Finally it can be possible to obtain the most-likely AE source locations and elastic wave velocity of each cell by iterating this process. This is the principle of ray-trace technique. In this way, unlike the conventional AE monitoring, we can obtain the AE source location considering the heterogeneity of the elastic wave velocity over the structures.

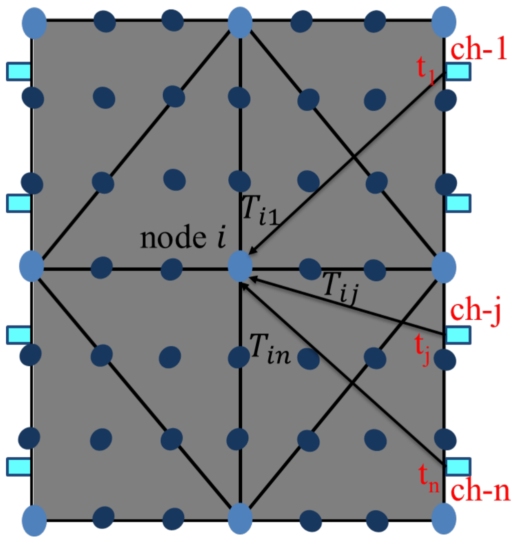

Fig. 4. Overview of ray-trace technique

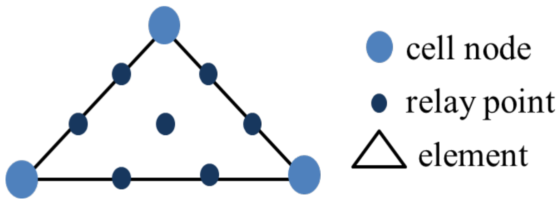

Fig. 5. Composition of an element

2.3 3D AE Tomography

In order to evolve this 2D AE tomography practically, 3D AE tomography has been proposed at present. Firstly the element in the 3D AE tomography is expressed in three dimensions different from the one of 2D AE tomography as shown in Fig. 6, where the most different point between 2D AE tomography and 3D AE tomography is the ray-trace technique in the algorism. In the developed ray-trace technique, the waves in 3D AE tomography are expressed by Eqs. 3 and 4, which are expanded to three dimensions different from Eq. 5 used in 2D AE tomography.

$$a_1\mathrm{x} + b_1\mathrm{y} + c_1 z + d_1 = 0 \tag{3}$$
$$a_2\mathrm{x} + b_2\mathrm{y} + c_2 z + d_2 = 0 \tag{4}$$
$$\mathrm{ax} + \mathrm{by} + \mathrm{c} = 0 \tag{5}$$

For the sake of this developed ray-trace technique, it can be possible to verify the AE source location and the deterioration of elastic wave velocity in 3 dimensions. In the past study, the applicability of 2D AE tomography was confirmed for a rock material. So the applicability of 3D AE tomography in this paper is verified with the same rock material as of the 2D's past study.

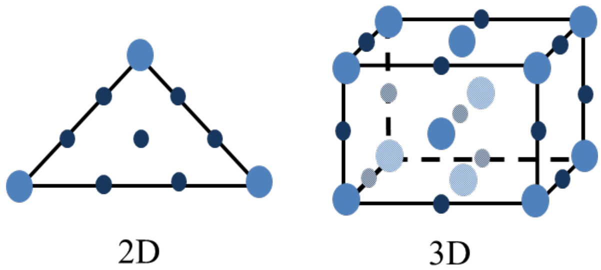

Fig. 6. Developed ray-trace technique

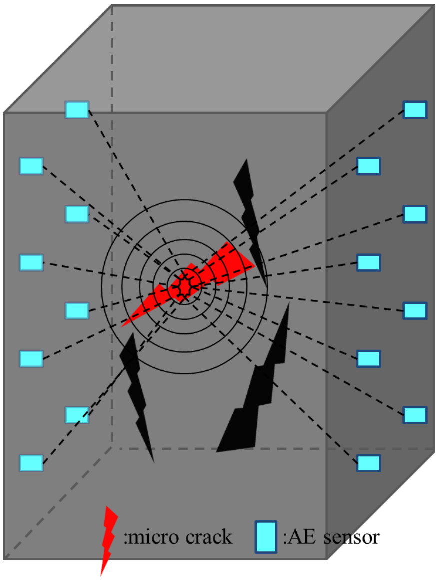

Fig. 7. The configuration of 3D AE tomography

3. Experimental Condition and the Result of 2D AE Tomography

3.1Experimental Condition and Sensor Arrangement

Cylindrical tuff specimens were sampled at the site of rock slope failure monitoring in Hokkaido, Japan. The specimen has 100 mm in diameter and 200 mm in height. The array of AE sensor for the AE tomography is shown as in Fig. 8. The plane surrounded by sensor 1, 2, 5 and 6 was referred to as ‘A-plane’, and the plane surrounded by sensor 3, 4, 7 and 8 was referred to as ‘B-plane’. Four strain gauges were installed onto the central surface of the specimen. Figure 9 shows the photos with regards to the triaxial compression test and the rock material. The triaxial compression tests were conducted under consolidated drained condition for generating AE activity in the specimen. The confining pressure was set at 294 kPa and the loading rate was kept constant by 1 kN/min. Finally, shear fracture was observed in the specimen as shown in Fig. 9 causing 907 AE events.

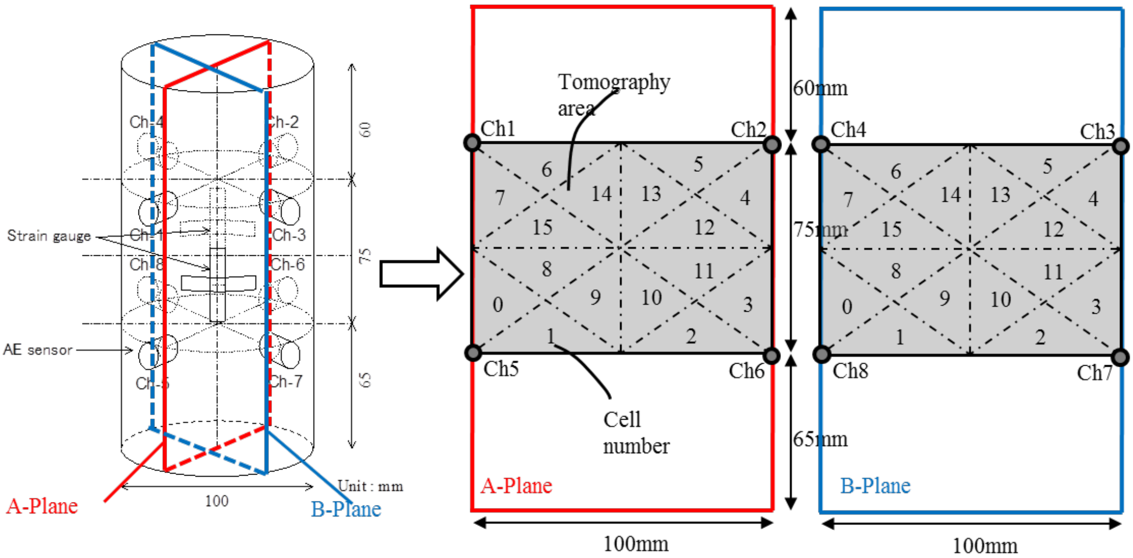

Fig. 8. Array of AE sensors

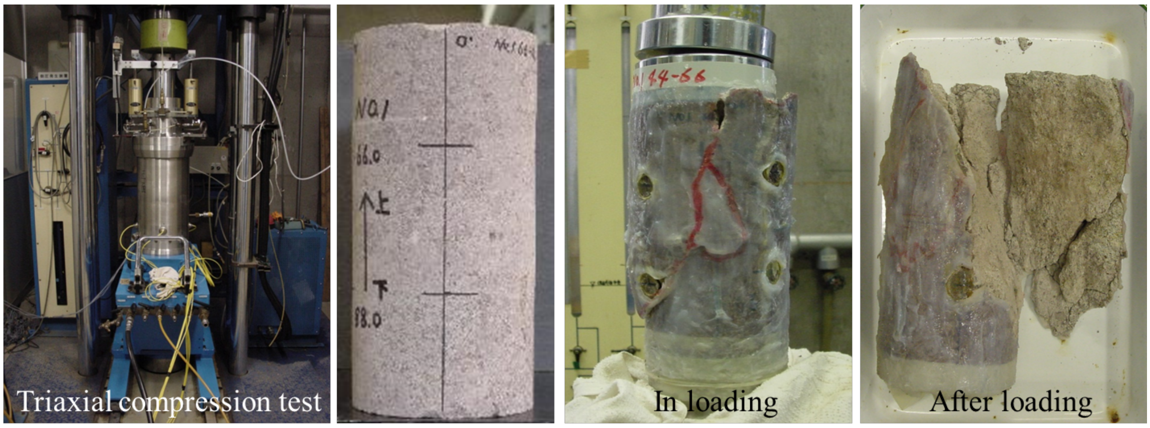

Fig. 9. Photos of rock material during loading and after the loading

3.2 The Result of 2D AE Tomography

Figure 10 shows the accumulated numbers of AE events and the transverse strain with elapsing time. As shown, the accumulated number of AE events is increasing along with increase of transverse strain. So there is a correlation between AE activities and the progress of rock fracture. Focusing on the relation between time and accumulated number of AE events, the state of fracture progress is divided into three stages. The stage from step-0 to step-1 is regarded as the progress stage of the microscopic failure. Then the stage from step-1 to step-2 is considered as of a steady stage of mesoscopic failure and the stage from step-2 to step-3 is one to be the final macroscopic failure. Then in order to verify the change of velocity structure in each stage, 2D AE tomography analysis was conducted for four steps from 0 to 3. The AE tomography can reflect the whole of the past-fracture/ damage phenomenon only with the most latest AE data, so that AE tomography analysis was conducted with 10 or 20 AE events data obtained around the end of the specific stage.

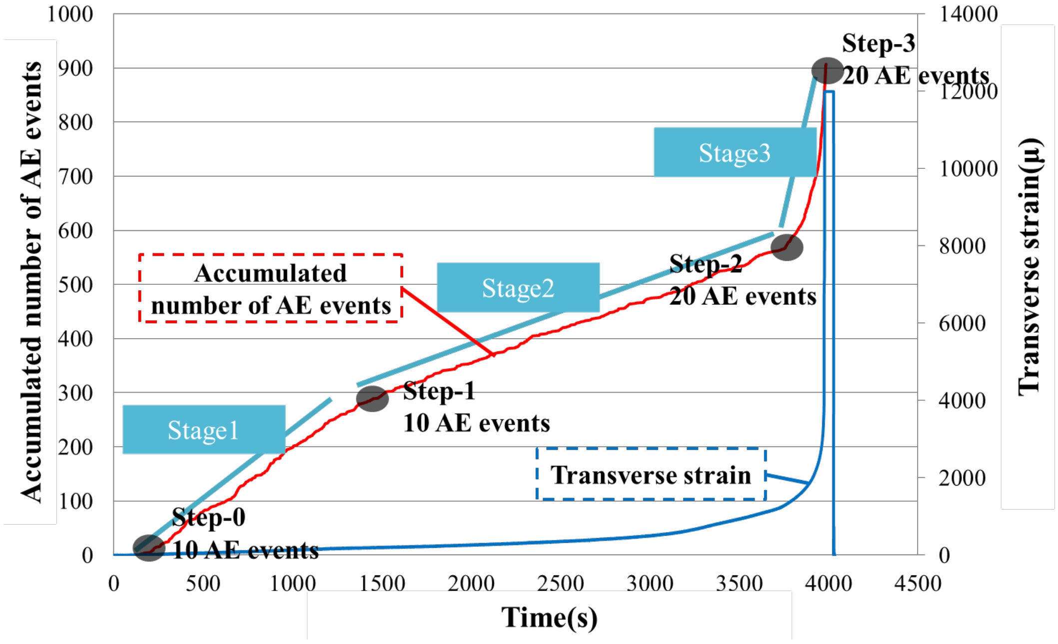

Fig. 10. Cumulative numbers of AE events and transversal strain over the experimental time

Figures 11 and 12 show the 2D tomograms in the A-plane and the B-plane, respectively. From Figs. 11-12, it is obvious that areas where a large number of AE events have emerged intensively do not always correspond to the areas exhibiting the low elastic wave velocity (see step 2 in Fig. 11 and step 3 in Fig. 12). For step-3 in both figures of 11 and 12 corresponding to the damage evolution up to step-3, a diagonal zone of low velocity can be found. This implies that internal damage evolves exponentially in stage-3 and this can be explained with the rapid increase of transversal strain from step-2 to step-3. Besides the assumed shear plane by AE tomography emerged during step 2-3 accorded well to the plane confirmed by the photo (see the right photo of Fig. 9). Accordingly it was possible to visualize the progress of the internal failure with the 2D AE tomography. However it is noted that the 2D AE tomography can evaluate only two specific planes such as A-plane and B-plane of the specimen, and therefore the 3D AE tomography is necessary to evaluate the whole failure process within the specimen. Hereby the 3D AE tomography has been developed and applied for this rock specimen to evaluate the 3D internal damage evolution.

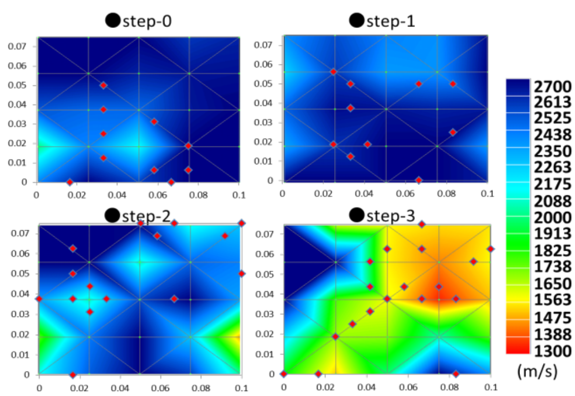

Fig. 11. Result of 2D AE tomography in A-plane

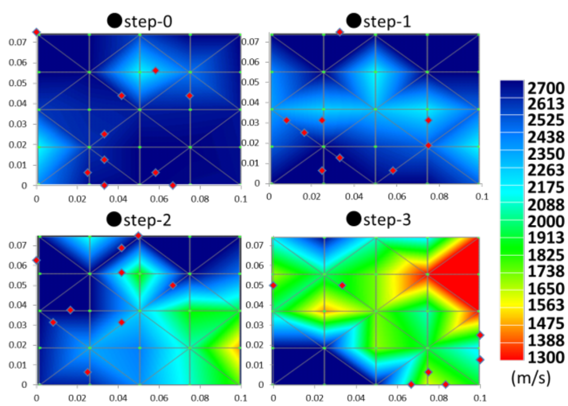

Fig. 12. Result of 2D AE tomography in B-plane

4. The Result of 3D AE Tomography

Figure 13 shows the AE source locations in the specimen in each step again. The blue plots show the AE source locations which have the peak amplitude larger than 50 dB, with the same manner, the green and yellow ones show the AE sources between 60 dB and 70 dB, between 70 dB and 80 dB respectively, and red ones show the AE sources larger than 80 decibel. It is obvious that the number of AE sources is increasing in accordance with the load application. Although the precise comparison shall been further examined, the plane comprised of red points in step-3 in Fig. 13 might be identical to the shear failure plane observed visually after the test.

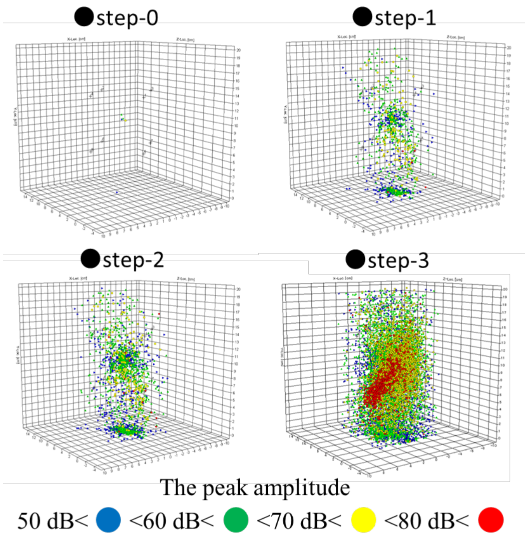

Fig. 13. AE sources in 3 dimension

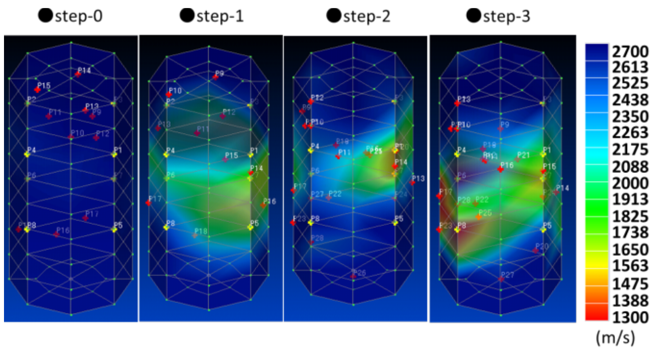

Fig. 14. Result of 3D AE tomography

The results of 3D AE tomography are shown in Fig. 14. The decrease areas of elastic wave velocity couldn't be confirmed in step-0, implying no remarkable damage progress in this step. In the following step-1 and step-2, the low elastic wave velocity was confirmed to develop in the central area of the specimen. From step-0 to step-1, the progress of damage was thus expected; however, from step-1 to step-2, obvious damage progress can't be verified presumably due to the stress re-distribution. While in the step-3, the large scale of damage evolution was apparent as the low elastic wave velocity was confirmed from the upper right area to the lower left area in the specimen, which is regarded as the final step of the failure. It is noted that this final damage evolution was in good accordance with the shear plane confirmed by both of visual observation and the result of AE source location in 3 dimensions.

5. Conclusions

In this paper, a rock material was subjected to triaxial compression test to evolve damage three dimensionally and to verify the applicability of 3D AE tomography. Through the AE sources and the damage evolution evaluated by the 3D AE tomography, the following results were obtained:

- Compared the results of 3D AE tomography with the AE sources in each step, it was clarified that evolution of the AE sources namely damage progress leads to the area expansion of the low elastic wave velocity in the specimen.

- From the result of step-3 in Fig. 14, implying the final stage of the failure, the low velocity area was confirmed from the upper right to the lower left exhibiting the formation of the shear plane. Considering the result of 2D AE tomography in Figs. 11 and 12, the photos of specimen's failure pattern in Fig. 9 and the AE sources in Fig. 13, the low velocity area might be the shear plane resulting in the eventual failure of the specimen. Correspondingly it was concluded that evaluation of the internal damage progress of rock materials was reasonably conducted with the 3D AE tomography.

References

[1] Matsui, S., Deck slab on road bridge, Morikita Publishing Corp., pp. 216-219, 2007.

[2] Shiotani, T., Okude, N., Momoki, S. and Kobayashi, Y., Proposal of AE tomography technique for the assessment of infrastructures, 18th National Conference on Acoustic Emission, pp. 39-42, 2011. (in Japanese)

[3] Kobayashi, Y., Shiotani, T. and Oda, K., Effects of number of events and relay point density on accuracy of three-dimensional AE-tomography, The 5th Asia and Pacific Young Researchers and Graduates Symposium, 2013.

[4] Osawa, S., Shiotani, T. and Ohtsu H., Visualization of damage in RC bridge deck for bullet trains with AE tomography, EIT-JSCE Joint International Symposium on International Human Resource Development for Disaster-Resilient Countries 2013, pp. 77-82, 2013.

[5] Iwamoto, K., Shiotani, T., Kobayashi, Y. and Momoki, S., Application of AE tomography for fracture visualization of rock material, Progress in Acoustic Emision XVI, pp. 193-198, 2012.

[6] Kobayashi, Y. and Shiotani, T., Seismic tomography with estimation of source location for concrete structures, Structural Faults and Repair 2012, Edinburgh, 2012.